Electrochimica Acta 55 (2010) 4926–4934

Contents lists available at ScienceDirect

Electrochimica Acta

journal homepage: www.elsevier.com/locate/electacta

Non-isothermal effects of single or double serpentine proton exchange membrane fuel cells

Xiao-Dong Wang[a,*], Xin-Xin Zhang[a], Wei-Mon Yan[b], Duu-Jong Lee[c,**], Ay Su[d]

[a] Department of Thermal Engineering, School of Mechanical Engineering, University of Science and Technology Beijing, Beijing 100083, China
[b] Department of Greenergy Engineering, National University of Tainan, Tainan 106, Taiwan
[c] Department of Chemical Engineering, National Taiwan University, Taipei 106, Taiwan
[d] Department of Mechanical Engineering, Fuel Cell Center, Yuan Ze University, Taoyuan 300, Taiwan

ARTICLE INFO

Article history:
Received 28 January 2010
Received in revised form 28 March 2010
Accepted 29 March 2010
Available online 4 April 2010

Keywords:
Proton exchange membrane fuel cell
Two-phase model
Serpentine flow field
Flow channel size

ABSTRACT

Mathematical models on transport processes and reactions in proton exchange membrane (PEM) fuel cell generally assume an isothermal cell behavior for sake of simplicity. This work aims at exploring how a non-isothermal cell body affects the performance of PEM fuel cells with single and double serpentine cathode flow fields, considering the effects of flow channel cross-sectional areas. Low thermal conductivities of porous layers in the cell and low heat transfer coefficients at the surface of current collectors, as commonly adopted in cell design, increase the cell temperature. High cell temperature evaporates fast the liquid water, hence reducing the cathode flooding; however, the yielded low membrane water content reduces proton transport rate, thereby increasing ohmic resistance of membrane. An optimal cell temperature is presented to maximize the cell performance.

1. Introduction

Proton exchange membrane fuel cells (PEMFCs) are regarded as promising alternative power-generation devices. Water management on the cathode side of a PEMFC is essential to determine power output of the cell [1–4]. An optimal flow field in the bipolar plates could uniformly distribute reactants over the fuel cell and sweeps the produced water out of the cell through the flow channels. Parallel, interdigitated, serpentine, and many other combined configurations of flow designs have been developed [5–46]. Geometric parameters of the serpentine flow field include active area, cross-sectional shape and area of the flow channels, width ratio of the flow channel to the rib, aspect ratio of the flow channel, number of serpentine loops, number of flow channel bends, and others [10].

Cell temperature significantly influences the cell performance. High cell temperature would increase the catalytic activity and decrease cathode flooding. However, a very high cell temperature may lead to membrane dehydration or even membrane dry-out, consequently retarding proton transport. The cell performance would be deteriorated at cell temperature higher than the humidification temperature [47–49].

The two-phase transport processes in non-isothermal PEMFCs with varying channel cross-sectional area and with single and double serpentine flow fields have not been satisfactorily studied. This work numerically evaluated the performance of a non-isothermal fuel cell with single or double serpentine flow fields at varying channel cross-sectional area. Cell performance and local distributions of current density, liquid water and cell temperature were evaluated. Effects of channel cross-sectional area and a non-isothermal cell assembly on cell performance were discussed.

2. Model and solution

Fig. 1 schematically shows the fuel cells presently studied, which comprises the anode flow channel, the anode gas diffusion layer, the anode catalyst layer, the proton exchange membrane, the cathode catalyst layer, the cathode gas diffusion layer, and the cathode flow channel. In the present study, the cell was kept at a fixed active area of 23 mm × 23 mm, and thickness of 0.35 mm for gas diffusion layer, 0.005 mm thickness of catalyst layer, and 0.035 mm thickness of proton exchange membrane. The anode flow channels were assumed to be in parallel with the channel and rib widths of 1 mm since the anode flow channel geometry has little effect on the cell performance. The cathode flow channels were assumed to be single or double serpentine flow fields having various flow channel cross-

* Corresponding author. Tel.: +86 10 62321277; fax: +86 10 81765088.
** Corresponding author. Tel.: +886 2 23625632; fax: +886 2 23623040.
E-mail addresses: wangxd99@gmail.com (X.-D. Wang), djlee@ntu.edu.tw (D.-J. Lee).

0013-4686/$ – see front matter
doi:10.1016/j.electacta.2010.03.092

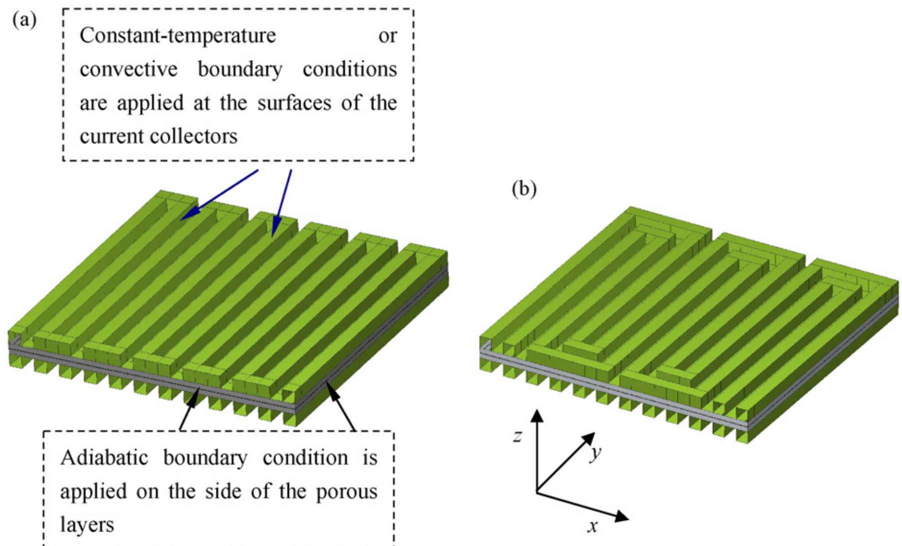

Fig. 1. Schematics of PEM fuel cells with single and double serpentine flow fields on the cathode and parallel flow field on the anode.

Table 1
Cathode channel sizes, inlet flow velocities, Reynolds numbers and pressure drops for the single and double serpentine flow fields with various cathode channel cross-sectional areas.

Flow field type	Cell	Channel cross-sectional area (mm^2)	$V_{in,c}$ ($m\,s^{-1}$)	Re	ΔP_{total}/Pa
Single serpentine	C8–R7	1.533 × 1.533	2.553	218.04	120.3
	C10–R9	1.210 × 1.210	4.098	276.24	304.4
	C12–R11	1.000 × 1.000	6.000	334.26	487.14
	C16–R15	0.742 × 0.742	10.900	450.57	965.9
	C22–R21	0.535 × 0.535	20.962	624.77	1557.1
Double serpentine	C8–R7	1.533 × 1.533	1.276	108.98	53.8
	C10–R9	1.210 × 1.210	2.049	138.12	158.4
	C12–R11	1.000 × 1.000	3.00	167.13	347.4
	C16–R15	0.742 × 0.742	5.450	225.29	928.6
	C22–R21	0.535 × 0.535	10.486	312.54	1850.3

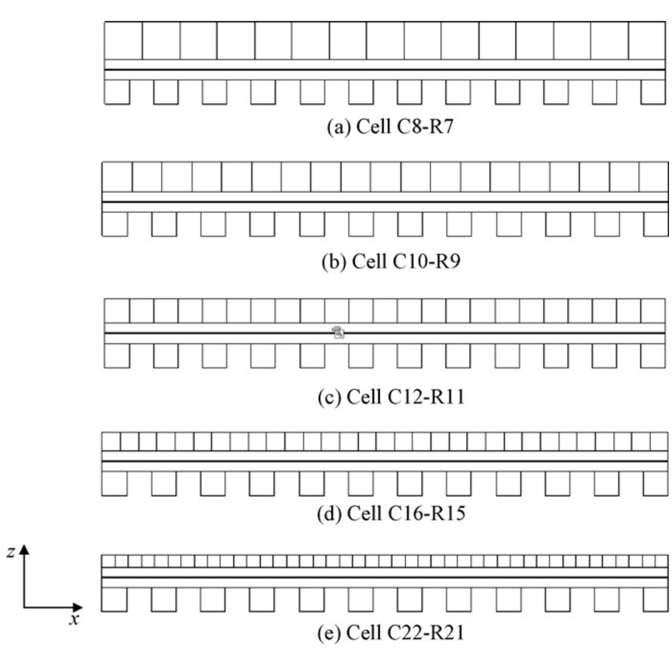

Fig. 2. Side view of PEM fuel cells with serpentine flow field.

Table 2
Value of key parameters in the model.

Parameter	Value
$\varepsilon_{channel}$	1
ε_{GDL}	0.5
ε_{CL}	0.4
ε_{MEM}	0.28
$k_{p,channel}$	∞
$k_{p,GDL}$	$1.76 \times 10^{-11}\,m^2$
$k_{p,CL}$	$1.76 \times 10^{-11}\,m^2$
$k_{p,MEM}$	$1.8 \times 10^{-18}\,m^2$
$\tau_{channel}$	1
τ_{GDL}	1.5
τ_{CL}	1.5
τ_{MEM}	Dagan model
$Aj_{0,a}^{ref}/\left(C_{H_2}^{ref}\right)^{0.5}$	$9.227 \times 10^{8}\,(A\,m^{-3})/(m^3\,kg^{-1}\,mol\,H_2)^{0.5}$
$Aj_{0,c}^{ref}/C_{O_2}^{ref}$	$1.05 \times 10^{6}\,(A\,m^{-3})/(m^3\,kg^{-1}\,mol\,O_2)$
α_a/α_c on the anode side	0.5/0.5
α_a/α_c on the cathode side	1.5/1.5
k_c	$100\,s^{-1}$
k_e	$100\,atm^{-1}\,s^{-1}$
σ	$0.0625\,N\,m^{-1}$
σ_s	$5000\,S\,m^{-1}$
$\sigma_{m,CL}$	$4.2\,S\,m^{-1}$
ρ_l	$1000\,kg\,m^{-3}$
ρ_{dry}	$1980\,kg\,m^{-3}$
μ_l	$3.65 \times 10^{-4}\,Pa\,s$
M_m	$1.1\,kg\,mol^{-1}$